Lifetime prediction of adhesive joints subjected to variable amplitude fatigue.

V. Shenoy [a], I. A. Ashcroft [a*], G. W. Critchlow [b],
A. D. Crocombe [c], M. M. Abdel Wahab. [c]

[a] *Wolfson School of Mechanical and Manufacturing Engineering, Loughborough University, LE11, 3TU, UK*

[b] *Institute of Polymer Technology and Materials Engineering (IPTME), Loughborough University, LE11, 3TU, UK*

[c] *School of Engineering (H5), University of Surrey, Guildford, Surrey, GU2 5XH, UK*

Abstract

Almost all structural applications of adhesive joints will experience cyclic loading and in most cases this will irregular in nature, a form of loading commonly known as variable amplitude fatigue (VAF). This paper is concerned with the VAF of adhesively bonded joints and has two main parts. In the first part, results from the experimental testing of adhesively bonded single lap joints subjected to constant and variable amplitude fatigue are presented. It is seen that strength wearout of bonded joints under fatigue is non-linear and that the addition of a small number of overloads to a fatigue spectrum can greatly reduce the fatigue life. The second part of the paper looks at methods of predicting VAF. It was found that methods of predicting VAF in bonded joints based on linear damage accumulation, such as the Palmgren-Miner rule, are not appropriate and tend to over-predict fatigue life. Improved predictions of fatigue life can be made by the application of non-linear strength wearout methods with cycle mix parameters to account for load interaction effects.

Key words: Fatigue, load interaction effects, mean load change, strength wearout, adhesives.

1 Introduction

In many applications adhesively bonded joints are being considered as replacements for conventional joining techniques, such as bolted or riveted joints, owing to their numerous advantages, including; high stiffness, good strength-to-weight ratio, ability to join dissimilar materials and more uniform stress distribution. However, certain disadvantages are also associated with adhesive bonding, such as limited operating range, environmental sensitivity and difficulty of disassembly. Another limiting factor in the wider application of adhesively bonded joints in structural applications is the difficulty in reliably predicting the in-service performance of bonded joints, leading to a tendency of over-conservative design. A critical aspect of predicting the in-service behaviour is consideration of the effect of the actual loading spectra seen by the joint. In most cases this will involve irregular cyclic loading, commonly known as variable amplitude fatigue (VAF). Prediction of the performance of bonded joints subjected to fatigue is a complex problem and a number of methods have been proposed, as reviewed in [1]. To date, most of the reported experimental and predictive studies of fatigue in bonded joints have been restricted to constant amplitude fatigue (CAF) in which a sinusoidal waveform of constant load or displacement amplitude and mean and constant frequency have been used. In most real applications these will all vary considerably in-service. Most of the previous studies of VAF in metals have shown crack growth retardation after overloads [2-4], however, there are also instances when crack growth accelerations in metals [5-7] and composites [8-10] have been seen. Studies on VAF in adhesively bonded joints have also reported accelerated failure [11-13]. This paper is concerned with the application of

various methods, based on total-life and strength wearout concepts, to predict the fatigue life of single lap joints subjected to VAF.

In the total life approach, the number of cycles to failure (N_f) is plotted as a function of a variable such as stress or strain amplitude. Where the loading is low enough that the deformation is predominantly elastic, a stress variable (S) is usually chosen and the resultant plot is termed an S-N curve, or Wöhler plot, and this is known as the stress-life approach. In bonded joints there is no unique relation between the easily measured average shear stress in a joint and the maximum stress. For this reason, load rather than stress is often used in total-life plots for bonded joints and hence these are known as L-N curves. In some cases efforts have been made to differentiate between the initiation and propagation phases in the S-N behaviour of bonded joints [14-18]. Shenoy et al [19] used a combination of back-face strain measurements and sectioning of partially fatigued joints to measure damage and crack growth as a function of number of fatigue cycles. It was seen from the sectioned joints that there could be extensive internal damage in the joint without external signs of damage; therefore, determination of an initiation phase from external observations alone is likely to lead to an overestimation. Shenoy et al. further, identified three regions in the fatigue life of an aluminium/epoxy single lap joint. An initiation period (CI) in which damage starts to accumulate, but a macro-crack has not yet formed, a stable crack growth (SCG) region in which a macro-crack has formed and is growing slowly and a fast crack growth region (FCG), which leads to rapid failure of the joint. They found that the percentage of life spent in each region varies with the fatigue load. At low loads the fatigue life is dominated by crack initiation, whereas crack

growth dominates at high loads. They also showed that the back-face strain signal associated with each phase of fatigue damage can be used to monitor damage in a bonded joint.

The S-N curve is only directly applicable to constant amplitude fatigue whereas in most practical applications for structural joints a variable amplitude fatigue spectrum is more likely. A simple method of using S-N data to predict variable amplitude fatigue is that proposed by Palmgren [20] and further developed by Miner [21]. The so called Palmgren Miner (PM) rule can be represented by:

$$\sum \frac{n_i}{N_{fi}} = 1 \qquad (1)$$

where n_i is the number of cycles in a constant amplitude block and N_{fi} is the number of cycles to failure at the stress amplitude for that particular block and can be obtained from the S-N curve. It can be seen that using Eqn. 1, the fatigue life of a sample in variable amplitude fatigue can be predicted from an S-N curve obtained from constant amplitude fatigue testing of similar samples. However, there are a number of serious limitations to this method, primarily, the assumptions that damage accumulation is linear and that there are no load history effects. Modifications to the PM rule have been suggested to address some of the deficiencies, e.g. [22-25], however, any improvements are at the expense of increased complexity and/or more testing and the basic flaw in the method, i.e. that it bears no relation to the actual progression of damage in the sample, is still not addressed. Erpolat et al. [12] used the PM law and the extended PM law, in which cycles below the

endurance limit also contribute to damage accumulation, to predict failure in an epoxy-CFRP double lap joint subjected to variable amplitude (VA) fatigue spectra. The resulting Miner's sum was significantly less than 1, varying between 0.04 and 0.3, and decreased with increasing load. This indicated that load sequencing was causing damage acceleration, i.e. that the PM rule was non-conservative.

An alternative phenomenological approach to the total life methods described above is to characterise fatigue damage as a function of the reduction in the strength or stiffness of the joint during its fatigue life. Stiffness wearout has the advantage of being non-destructive, however, it is not directly linked to a failure criterion and may not be very sensitive to the early stages of damage. The strength wearout method provides a useful characterisation of the degradation of residual strength but requires extensive destructive testing. In the strength wearout method the joint's strength is initially equal to the static strength, S_u, but decreases to $S_R(n)$ as damage accumulates through the application of n fatigue cycles. This degradation can be represented by:

$$S_R(n) = S_u - f(S_u, S_{\max}, R)n^{\kappa} \qquad (2)$$

where κ is a strength degradation parameter, S_{max} is the maximum stress and R is the ratio of minimum to maximum stress (i.e. $R=S_{min}/S_{max}$). Failure occurs when the residual strength equals the maximum stress of the spectrum, i.e. when $S_R(N_f) = S_{max}$.

Schaff and Davidson [9, 10] extended Eqn. (2) to enable the residual strength degradation of a sample subjected to a variable amplitude loading spectrum to be predicted. However,

they noted a crack acceleration effect in the transition from one constant amplitude (CA) block to another, a phenomenon they termed the cycle mix effect, and proposed a cycle mix factor, CM, to account for this. Erpolat et al. [12] proposed a modified form of Shaff and Davidson's cycle mix equation to model the degradation of CFRP-epoxy double lap joints subjected to a variable amplitude fatigue spectrum. They showed that this model represented the fatigue life of bonded joints under variable amplitude fatigue more accurately than Palmgren-Miner's law.

Sectio 2 of this paper presents the results from an experimental investigation of VAF in adhesively bonded single lap joints. Section 2 goes on to examine various methods of predicting fatigue life and strength wearout in bonded joints.

2.0 Experimental

2.1 Materials and joint preparation

Single lap joints were prepared to the dimensions specified in British standard BS 2001 [26], as shown in Fig. 1. The adherends were cut from 0.2 and 0.3 mm thick sheets of Clad 7075-T6 aluminium alloy. The adhesive used was the toughened epoxy film adhesive FM 73M, supplied by Cytec Engineered Materials.

The adherends were ultrasonically cleaned in an acetone bath for five minutes prior to pre-treatment using a patented ACDC anodisation process [27]. This treatment is proposed as an environmentally friendly alternative to current chromate containing processes. The adherend to be treated is one of the electrodes in an electrochemical cell.

A mixture of phosphoric and sulphuric acid (5%) is used as the electrolyte and the other electrode is titanium. An alternating current (AC) is ramped up to 15V over a period of 1 minute and then kept at this voltage for two more minutes. The current is then changed to direct current (DC) and increased to 20V and kept at this voltage for 10 minutes. The adherends are then washed with distilled water and dried in hot air. This pre-treatment results in an average oxide thickness of 1.9μm over the adherend surface, as shown in Fig. 2(a). In this figure two layers are apparent; the bottom layer is the aluminium cladding layer and the top layer is the oxide layer. A magnified image of the surface of the oxide film is shown in Fig. 2(b), where the open pored structure required for good bonding can be seen. An advantage of the ACDC process is that in addition to the open structure at the surface, produced during the AC phase, a denser structure is produced in the DC phase, which results in enhanced corrosion protection of the aluminium alloy. After the ACDC pre-treatment, a thin film of BR 127 corrosion resistant primer, manufactured by Cytec Engineered Materials Ltd., was applied to the aluminium adherends. This was dried at room temperature and then cured at 120°C for half an hour. The adherends were returned to room temperature before bonding. The FM 73M adhesive was taken from freezer storage and brought to room temperature in a dry atmosphere before bonding. The adhesive was cured at 120°C for one hour, with constant pressure applied through clips. No attempt was made to control the fillet geometry but owing to the accurate cutting of the film adhesive the natural fillets formed were fairly uniform between samples. The bonded joints were stored in a dessicator at room temperature prior to testing.

2.2 Quasi-static and constant amplitude fatigue (CAF) testing

The results in this section have been reported previously [19, 28] but are repeated as they are necessary for the predictive methodologies reported in section 3. These references should be used if further details of the testing procedures or interpretation of results are required. All tests were carried out under ambient laboratory environmental conditions, in which temperature ranged from 22-25°C and relative humidity ranged from 35-40% during the tests. An Instron 6024 servo-hydraulic testing machine was used for all the testing. Quasi-static testing was carried out at a constant displacement rate of 0.1mm/sec. The mean quasi static failure load (QSFL) of the 5 samples tested was 11.95kN, with a standard deviation of 0.31.

Joints were fatigue tested in load control using a sinusoidal waveform with a load ratio of 0.1 and frequency of 5Hz. Various percentages of the quasi-static failure load (QSFL) were taken as the maximum load in the fatigue spectrum. A plot of maximum load against the number of cycles to failure from these tests is shown in Fig. 3. A linear fit to the data is seen in which the standard deviation is 1.6.

In addition to carrying out fatigue tests to complete failure, as described above, partial fatigue testing of joints was also carried out, in order to measure strength wearout. Joints with similar sized fillets were tested for a certain number of fatigue cycles, and then loaded quasi-statically to measure the residual strength in the joint. Strength wearout is expressed in terms of the QSFL needed to fail the joint after it has been fatigue tested for a certain number of cycles. This is termed the residual load, $L(n)$. The results of this

testing are shown in Fig. 4(a). Non-linear strength wearout can be seen for all loads and the data has been fitted to curves of the following form:

$$L(n) = L_f - (L_f - L_{\max})(n)^{v} \tag{3}$$

Where L_f is the quasi-static failure load prior to fatigue testing, L_{max} is the maximum fatigue load, n is the number of cycles the sample has been fatigue tested and v is an empirical curve fitting parameter. The curves end at the point, where the residual load has decreased to the maximum load in the applied fatigue load spectrum as quasi-static failure will occur at this point. This relationship is termed the non-linear strength wearout (NLSW) model in this paper. Fig. 4 (b) shows the data from Fig. 4(a) re-plotted with number of fatigue cycles before quasi-static testing (n) normalised with respect to the number of fatigue cycles to failure (N_f). Hence the normalised number of cycles is defined as $N_n=n/N_f$. Similarly the residual load ($L(n)$) is normalised with respect to the failure load of samples before fatigue testing (L_f), giving $L_n=L(n)/L_f$. It can be seen in Fig. 4(b) that a single curve, of the following form, now provides a reasonable fit to all the data, regardless of the fatigue load.

$$L_n = 1 - (\frac{L_f - L_{\max}}{L_f})(N_n)^{v} \tag{4}$$

This relationship is termed the normalised non-linear strength wearout model (NNLSW) model in this paper. This is a potentially significant relationship in terms of lifetime prediction, as discussed in Section 3.5.

The initiation and growth of damage and cracking in single lap joints subjected to fatigue loading has been discussed in previous papers [19, 28]. Fig. 5 shows a plot of crack/damage length ζ against number of cycles, n, for three different fatigue loads from data in these previous papers. A non-linear curve can be fitted to these points, representing a fatigue load dependent representation of damage evolution.

2.3 Variable amplitude fatigue (VAF) testing

VAF loading was achieved in this work by changing the mean load whilst maintaining a constant load ratio of 0.1. This method was principally chosen to aid the investigation of lifetime prediction as the constant amplitude data to be used in the predictive methods was obtained with a load ratio of 0.1. A constant frequency of 5Hz was used for the same reason. Fig. 6 shows two stages of a VAF load spectrum. In the spectrum a constant amplitude block of n_1 cycles with a mean load of L_{mean1} and maximum load of L_{max1} is alternated with a block of n_2 cycles with mean and maximum loads of L_{mean2} and L_{max2} respectively. Two main types of spectra where investigated, as characterised by different values of n_1 and n_2. In Type A spectra n_1=10 and n_2= 5 whereas in Type B spectra n_1=1000 and n_2 =5. For both of these spectra, various maximum loads and changes in mean load were investigated. Table 1 details all the loading permutations investigated. Three samples were tested for each of the loading conditions given in the table.

A comparison of the results from the CAF and VAF tests in terms of L_{max1} can be seen in Fig. 7. Type A spectra have 30% of the cycles as overloads compared to L_{max1}, with mean load increases of 18.75 to 40%, as described in Table 1. This has the effect of reducing

the mean fatigue life from between 83 to 91%, with the largest decrease coinciding with the greatest increase in mean load increase in the overloads. Type A spectra have only 0.5% of the cycles as overloads, however, this still has a significant effect on the fatigue life when the overloads are 23 and 40%, reducing the average fatigue life by 80 and 77%, respectively. However, there is relatively little effect on fatigue life when the increase of the mean load in the overloads is 18.75%.

3.0 Fatigue Lifetime Prediction

The following six different methods were used to predict fatigue lifetime under VAF.

a) Palmgren-Miner rule (PM)
b) Non-linear strength wearout (NLSW) model
c) Cycle mix (CM) model
d) Modified cycle mix (MCM) model
e) Normalised cycle mix (NCM) model
f) Modified normalised cycle mix (MNCM) model

These methods, and the results obtained from applying then to the data in Section 2 of the paper, are described in the following sections.

3.1 Palmgren-Miner (PM) rule

This method is described in Section 1 of the paper. In this case the L-N curve shown in Fig. 3 was used to predict the fatigue life of the samples subjected to VAF. The results are shown in Fig. 8. It can be seen that at low cycles the PM rule provides a reasonable prediction, however, at higher cycles the method over-predicts the fatigue life. This is

consistent with previous work [11-13] and indicates the acceleration of damage/cracking due to load interaction effects.

3.2 Non-linear strength wearout (NLSW) model

This approach to fatigue lifetime prediction is based on the strength wearout curves from CAF testing, such as those shown in Fig. 4. The assumed relationship between the residual load, $L(n)$ and normalised number of cycles is given in Eqn (3) where the parameter ν indicates the nature of strength wearout, as illustrated schematically in Fig. 9. A linear strength wearout (i.e. $v>1$) was assumed by Eroplat et al in [12], whereas Shenoy et al fitted curves with $v>1$ to their experimental data in [28]. The simplest method of using strength wearout curves from CAF tests to predict strength wearout and cycles to failure in samples subjected to VAF is illustrated in Fig. 10. Consider an initial block of CAF where the maximum fatigue load is L_{max1}. Residual load will follow the path a-b, as predicted using Eqn. 3, with an empirically determined value of v. If the maximum load is then increased to $L_{max2,}$ and no load interaction effects are assumed, the residual load will follow path b-c, indicating a switch to a different strength wearout curve without any decrease in the residual load. Strength wearout will then follow curve c-d. This can also be predicted using eqn. (3), but with a different value for v. This can be repeated, moving horizontally between strength wearout curves until the residual load has decreased to the value of L_{max}, at which point quasi-static failure occurs. The method can be extended to as many different strength wearout curves as are necessary to represent the VAF spectrum.

Figure 11 (a) show the CAF strength wearout curves required to predict the VAF behaviour described in Table 1. Where experimental strength wearout data was not available, strength wearout curves were estimated by interpolating between the existing strength wearout curves. In Fig. 11(b) strength wearout for CAF with L_{max} equal to 5kN is compared to that for with Type A and B VAF spectra with L_{max1} of 5kN. Quasi-static failure in the case of the VAF occurs when the residual load has reduced to that of the maximum load in the spectra. In the case of Type A and B VAF in Fig. 11 (b) this is at L_{max} =7kN. Preceding quasi-static failure, it can be seen that Type A VAF follows the AF fairly closely, whereas, residual load decreases much more quickly for Type A fatigue. This is to be expected considering 30% of the Type A spectra is composed of overloads, compared with only 0.1 % for Type B.

Fig. 12 shows the predicted L-N curves using the NLSW approach. These are a better fit to the data than the PM rule but show some similar trends, i.e. tendency to over prediction of fatigue life, especially at high cycles. This is further evidence of the existence of load interaction effects leading to crack/damage growth acceleration. Sections 3.3-3.6 introduce predictive methods in which these interaction effects are accounted for.

3.3 Cycle mix (CM) model

Erpolat et al. [12] developed a linear cycle mix (LCM) model to account for load interaction effects due to mean load change in a VAF spectrum. They used a linear form for the strength degradation, i.e. v=1 in Eqn. (3). It was assumed that mean load changes

caused a decrease in the residual load. This effect was accounted for by the introduction of a cycle mix parameter, *CM*, of the following form:

$$CM = \alpha \left[(\Delta L_{mn})^{\beta L_{\max} (\Delta L_{\max,} / \Delta L_{mn},)^{\gamma}} \right] \tag{5}$$

ΔL_{mn} and ΔL_{max} are the mean and maximum load changes during the transition from one mean load to the other, α and β are experimentally determined parameters and γ is assumed to be unity in this case. The application of the cycle mix factor to predict strength wearout and cycles to failure for VAF is illustrated in Fig. (13). In this case the CM factor was only applied when the mean load was increased as this produced the best fit to the data, however, in other cases application to decreases in load mean may be applicable.

In the absence of experimental data, Erpolat et al [12] assumed a linear strength wearout, however, in this case, as shown in Fig. (4), it was seen that a non-linear strength wearout curve provided a better fit to the experimental strength wearout data. Hence the prediction of strength wearout and fatigue life was based on non-linear strength wearout, as represented by Eqn. (3), combined with the cycle mix factor in Eqn. (5). This approach is termed the cycle mix (CM) model in this paper.

The predicted residual load decrease using the CM method is compared with that using the NLSW approach in Fig. 14. It can be seen that including the CM parameter greatly accelerates the predicted strength wearout for the Type A spectra but has less effect on

Type B. This can be attributed to the higher frequency of mean load changes in the Type A spectra (one in 15 cycles, compared with one in 1005 for Type B).

The predicted L-N curves using the CM approach are shown in Fig. 15. It can be seen that by accounting for load interaction effects by introduction of the CM parameter, a significantly better fit to the experimental data is seen than in the previous approaches in which load interaction effects are ignored. The CM parameter has had the desired effect of eliminating the over-prediction of fatigue life seen with the previous methods; however, there is still the potential to provide a better fit to the experimental data over the complete range of data. One of the limitations of the CM approach is that the CM parameter is assumed to be constant over the fatigue life of the joint. This may not be the case in reality, and hence the case of a variable cycle mix parameter is investigated in the next method.

3.4 Modified cycle mix (MCM) model

In the modified cycle mix (MCM) approach, a variable cycle mix parameter is introduced. Looking at the fit of the CM method with the constant CM parameter to the experimental data in Fig. 15 it can be seen that the predicted L-N curves provide a reasonable agreement across the range of cycles tested but don't capture the shape of the data particularly well. It can be seen that a better fit to the data would be acquired if the cycle mix factor was greater in the low cycle regime than in the high cycle regime. It has been seen in previous work that the fatigue life is propagation dominated in the low cycle regime and initiation dominated in the high cycle regime, hence, a possible way of

achieving the desired effect in a variable cycle mix parameter would be to make it dependent on the extent of damage in the sample, as introduced in Eqn. (6).

$$CM_m = \left(\frac{\zeta}{OL} + \alpha \right) \left[(\Delta L_{mn})^{\beta L_{max} (\Delta L_{max,} / \Delta L_{mn,})^{\gamma}} \right] \tag{6}$$

where, OL is the overlap length and ζ is a damage parameter. In this work ζ was determined by fitting a power law curve to the experimental plots of damage/crack growth vs. number of cycles curves shown in Fig. 5. Hence, ζ is defined as:

$$\zeta = m_1 (n)^{m_2} \tag{7}$$

Predicted strength wearout using the MCM approach is compared with that using the NLSW method in Fig. 16. By comparison with Fig. 15, it can be seen that the MCM method tends to result in a reduced load interaction effect compared to the CM method.

The predicted L-N curves using this approach are compared with the experimental values in Fig. 17. The prediction of fatigue life is similar to that using the CM approach in the low cycle regime but predicts a longer life in the high cycle regime, as desired. The resultant L-N curves appear to follow the trend seen in the experimental data slightly better than the CM approach, especially for Type A VAF. There is still scope to further improve the method, however, with this particular data set a better fit to the experimental data may be achieved most easily by imposing a fatigue threshold value as an asymptote for the L-N curve.

3.5 Normalised cycle mix (NCM) model

In the NLSW and CM methods, strength wearout curves were determined for each fatigue load using Eqn. (3), with load dependent curve fitting parameters. However, it can be seen in Fig 4(b) that a reasonable fit to all the strength wearout data, regardless of fatigue load, can be obtained by the application of Eqn. (4), which provides a relationship between normalised load and cycles. Basing strength wearout on Eqn. (4) rather than Eqn. (3) has the advantage that only a single, load independent experimental parameter is required to characterise strength wearout. Basing the prediction of VAF on Fig. (4) follows a similar method to that already described for the NLSW method, except a single normalised strength wearout curve is used. This can be used without a cycle mix parameter, if interaction effects are ignored, as in the NLSW approach, or with the constant or variable cycle mix parameters introduced in Eqns. (5) and (6). It has already been seen that ignoring load interaction effects results in an over prediction in fatigue life for the joints and VAF spectra in this work and hence the normalised strength wearout method has used with the constant cycle mix parameter of Eqn. (5) or the variable cycle mix parameter of Eqn. (6). The two approaches are termed the normalised cycle mix (NCM) and modified normalised cycle mix (MNCM) model respectively. The prediction of L-N curves using both approaches can be seen in Fig. 19. It can be seen that there is little difference between the two methods and that both provide a good fit to the experimental data.

4 Discussion

In the first part of this paper, results from the constant and variable amplitude fatigue testing of adhesively bonded single lap joints were presented. It was seen that in constant amplitude testing a plot of failure load against the logarithm of number of cycles to failure (L-N plot) could be represented by a straight line fit to the experimental data. Strength wearout measurements showed a non-linear decrease in the residual failure load of fatigue tested samples, with an acceleration towards the end of the fatigue life, which coincided with a rapid increase in the damage in the sample. This non-linear degradation means that predictive methods based on linear damage accumulation, such as Palmgren-Miners law, may not be appropriate. It was also seen that when normalised failure load was plotted against normalised number of cycles that all the strength wearout data, regardless of fatigue load, could be represented by a single curve. This is significant for failure prediction as it reduces the number of experimentally determined constants required for life prediction and allows easy accommodation of the prediction of fatigue lives including loads not covered by the experimental strength wearout tests. In the variable amplitude fatigue testing, two main types of spectra were investigated, the difference being the proportion of the fatigue life at higher loads. It was seen that the introduction of only small numbers of cycles at higher loads could result in a large decrease in the number of cycles to failure. This is in agreement with previous work, which has indicated load interaction effects in the variable amplitude fatigue testing of bonded joints, with both mean load changes and overloads resulting in damage acceleration [11-13]. These effects need to be accommodated in any lifetime prediction

procedure if the variable amplitude fatigue behaviour of adhesively bonded joints is to be accurately predicted.

In the second part of the paper a number of methods of predicting the VAF response of adhesively bonded joints were investigated. The first model was the well known Palmgren-Miners (PM) law. The advantage of this method is that fatigue life can be predicted using only the L-N curve from constant amplitude fatigue testing. The disadvantages are that the method doesn't account for non-linear damage accumulation or load interaction effects. Application of this method resulted in an over-prediction of fatigue life, particularly at high cycles, in agreement with previous work [12].

All the other lifetime prediction methods were based on strength wearout measurements. These methods have the advantage over the PM rule that non-linear degradation is easily accounted for; however, the experimental testing is more difficult. In the first application of strength wearout curves to predict VAF, load interactions were ignored. Lifetime prediction was better than the PM rule at high cycles but there was still a tendency to over-predict the fatigue life. The next development was to account for load interaction effects by utilising a cycle mix parameter to accelerate damage when the mean load changed. A constant cycle mix parameter was successful in reducing the predicted cycles to failure, but resulted in under-predicting the fatigue life at high cycles. An attempt to rectify this was made by introducing a cycle mix parameter that was dependent on damage in the sample. This improved the fit to the experimental data, but at the expense of increased complexity and further experimental testing. A final method attempted to

balance accuracy with simplicity by using the normalised strength wearout curve. It was seen that a reasonably good prediction of fatigue life could be made using the normalised strength wearout curve with a constant cycle mix parameter. This provided a good compromise between the capabilities of the method with ease of implementation.

5 Conclusions

Experimental testing has shown that the degradation of adhesively bonded joints in fatigue testing can be non-linear and that load interaction effects in variable amplitude fatigue can result in damage acceleration. This means that methods of predicting variable amplitude fatigue in bonded joints using methods based on linear damage accumulation, such as the PM rule, are not appropriate and tend to over-predict fatigue life. Improved predictions of fatigue life can be made by the application of non-linear strength wearout methods with cycle mix parameters to account for load interaction effects. The strength wearout methods have the further advantage that residual strength of the joint throughout the fatigue life can be predicted and, with the aid of further testing, can be related to physical damage in the sample and non-destructive measurements, such as back-face strain [28].

6 References

1. Ashcroft IA and Crocombe AD. Ed. A. Oechsner and L.F.M. da Silva, Springer Publishing, Chapter 7: Fatigue, 2008.

2. Sadananda K, Vasudevan AK, Holtz RL and Lee EU. Int. J Fatigue 1999; 21: 233-246.

3. Borrego LP, Ferreira JM and Pinho da Cruz JM, Costa JM. J Engineering Fracture Mechanics 2003; 70(11):1379-1397.

4. Viggo Tvergaard. Int. J fatigue 2005; 27:1389-1397.

5. Chang JB, Szamossi M and Liu KW. Eds.Chung JB, Hudson CM, editors. ASTM STP 748. USA ASTM 1979: 115–32.

6. Agerskov H. J Constr Steel Res. 2000; 53: 283–305.

7. Nisitani H and Nakamura K. Trans Japan Soc Mech Eng. 1982; 48: 990.

8. Farrow IR. PhD thesis. vols. 1 and 2, Cranfield Institute of Technology, 1989.

9. Schaff JR and Davidson BD. J Compos Mater. 1997; 31(2): 128–57.

10. Schaff JR and Davidson BD. J Compos Mater. 1997; 31(2): 158–81.

11. Erpolat S, Ashcroft IA, Crocombe AD and Abdel-Wahab MM. Comp. A. 2004; 35: 1175-1183.

12. Erpolat S, Ashcroft IA, Crocombe AD and Abdel-Wahab MM. Int. J. Fatigue 2004; 26: 1189-1196.

13. Ashcroft IA. J. Strain Anal. 39 2004; 707-716.

14. Harris JA and Fay PA. Fatigue life evaluation of structural adhesives for automotive applications. Int J Adhesion and Adhesives 1992; 12: 9-18.

15. Zhang Z and Shang JK. A backface strain technique for detecting fatigue crack initiation in adhesive joints. J Adhesion 1995; 49: 23-36.

16. Crocombe AD, Ong AD, Chan CY, Abdel Wahab MM and Ashcroft IA. J Adhesion 2002; 78: 745-778.

17. Graner-Solana A, Crocombe AD, Wahab MA and Ashcroft IA. J Adhesion Sci and Tech 2007; 21: 1343-1357.

18. Quaresimin M and Ricotta A. Int J Fat 2006; 28: 1166-1176.

19. Shenoy V, Ashcroft IA, Critchlow GW, Crocombe AD and Abdel Wahab MM. Int J Adhesion and Adhesives, 2008; in press.

20. Palmgren A. Die Lebensdauer von Kugellargen, Zeitschrift des Vereins Deutscher Ingenieure 1924; 68: 339-41.

21. Miner MA. Cumulative damage in fatigue. J Appl Mech 1945; 12: 159-64.

22. Marco SM and Starkey WL. A concept of fatigue damage. Trans Amer Soc Mech Engineers 1954; 76: 626-662.

23. Leve HL. Cumulative damage theories. In: Metal Fatigue: Theory and Design, John Wiley & Sons Inc, NY, USA 1969: pp 170-203.

24. Owen MJ and Howe RJ. J Physics D 1975; 5: 1637-1649.

25. Bond IP. Fatigue life prediction for GRP subjected to variable amplitude loading. Composites Part A 1999; 30: 961-970.

26. British Standard BS ISO (4587:2003).

27. Critchlow G, Ashcroft I, Cartwright T and Bahrani D, Anodising aluminium alloy, UK patent no. GB 3421959A.

28. Shenoy V, Ashcroft IA, Critchlow GW, Crocombe AD and Abdel Wahab MM. Int J Fatigue. in press.

Table 1. Different fatigue loads tested for VAF testing program.

L_{max1}	L_{max2}	n_1	n_2	% increase in mean load
5	7	10	5	40
5	7	1000	5	40
6.5	8	10	5	23
6.5	8	1000	5	23
8	9.5	10	5	18.75
8	9.5	1000	5	18.75

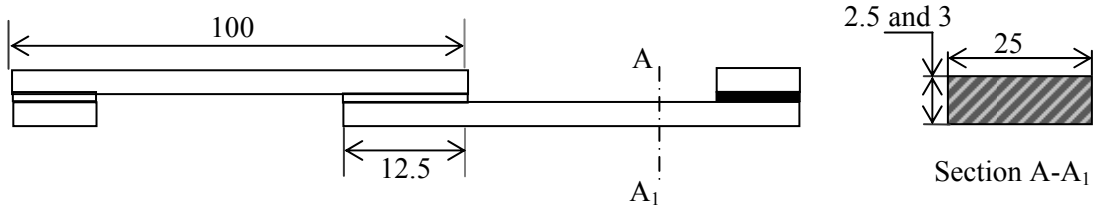

Fig. 1. SLJ geometry (dimensions in mm).

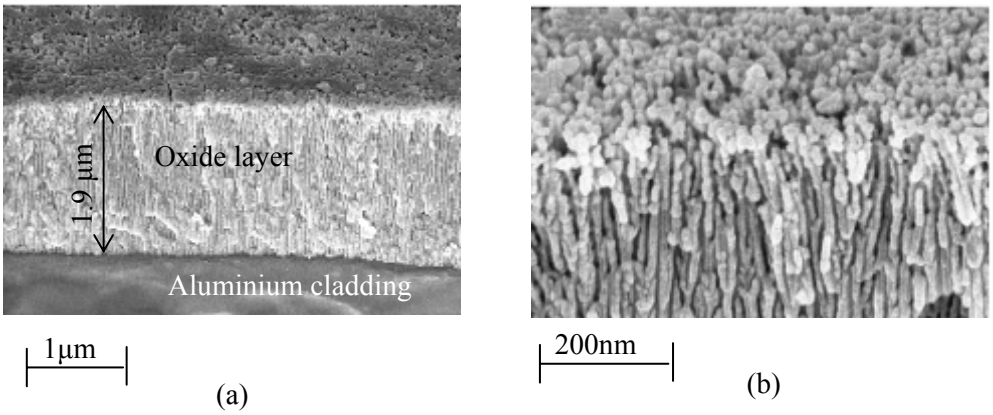

Fig. 2. Electron micrographs showing (a) the aluminium oxide layer formed during the AC DC pre-treatment and (b) a magnified image of the porous surface structure.

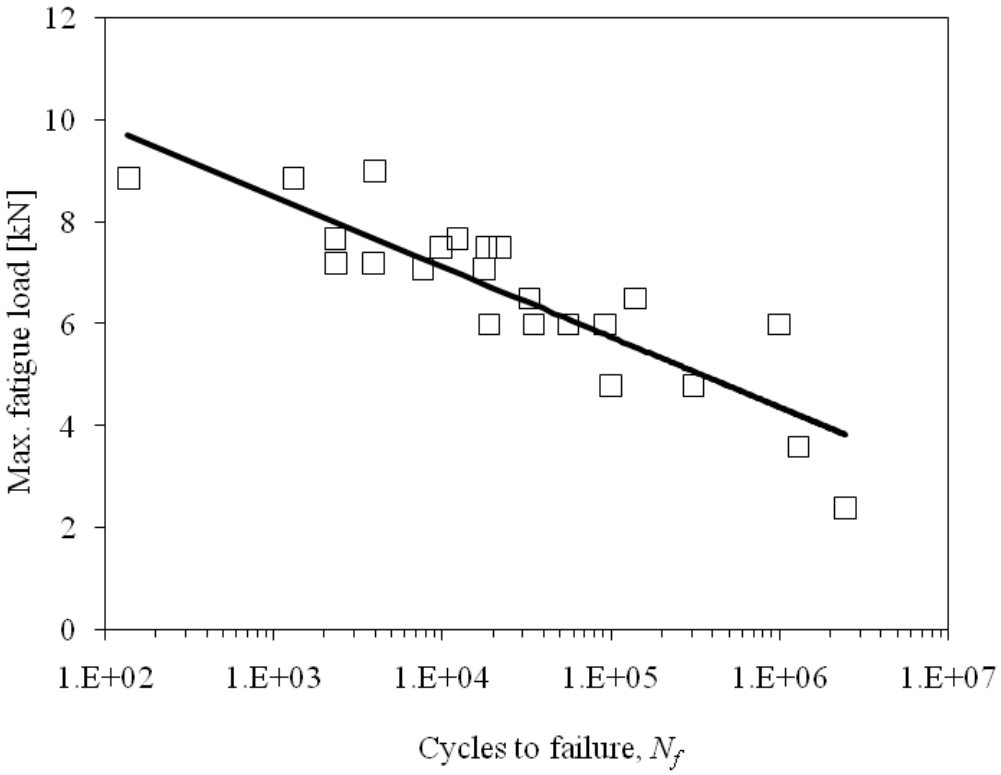

Fig. 3. L-N curve for the adhesively bonded single lap joints.

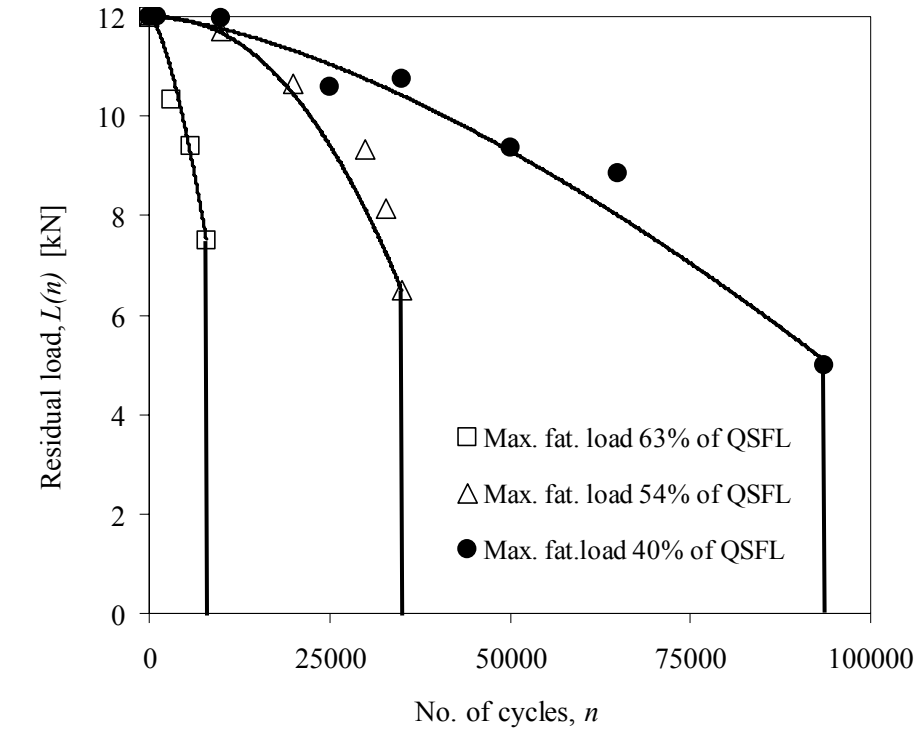

(a)

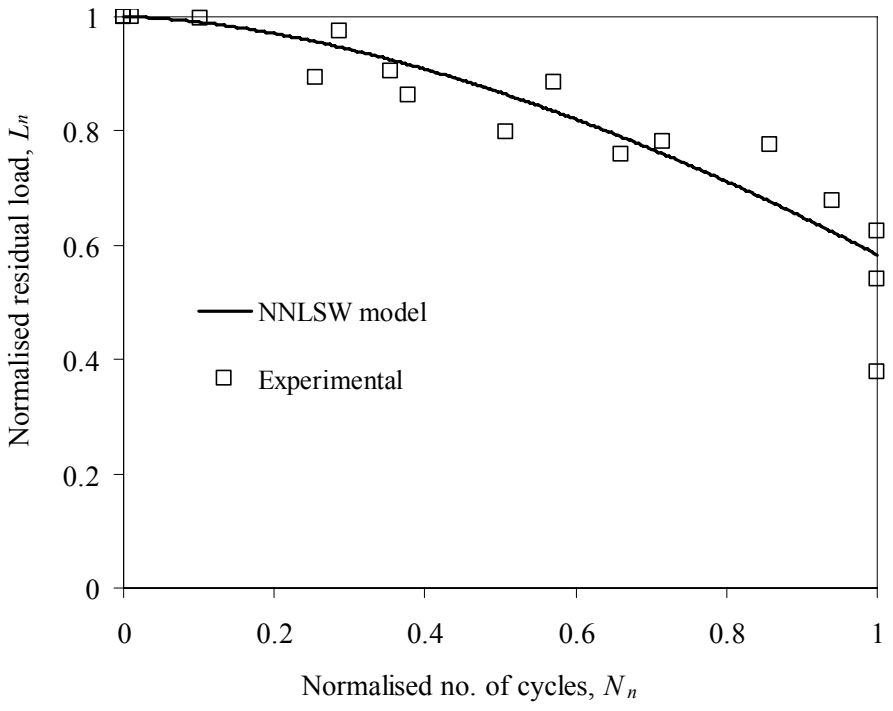

(b)

Fig. 4. (a) Strength wearout plots, with line fits using Eqn. (3) (b) Normalised strength wearout plot with data fitted to Eqn. (4).

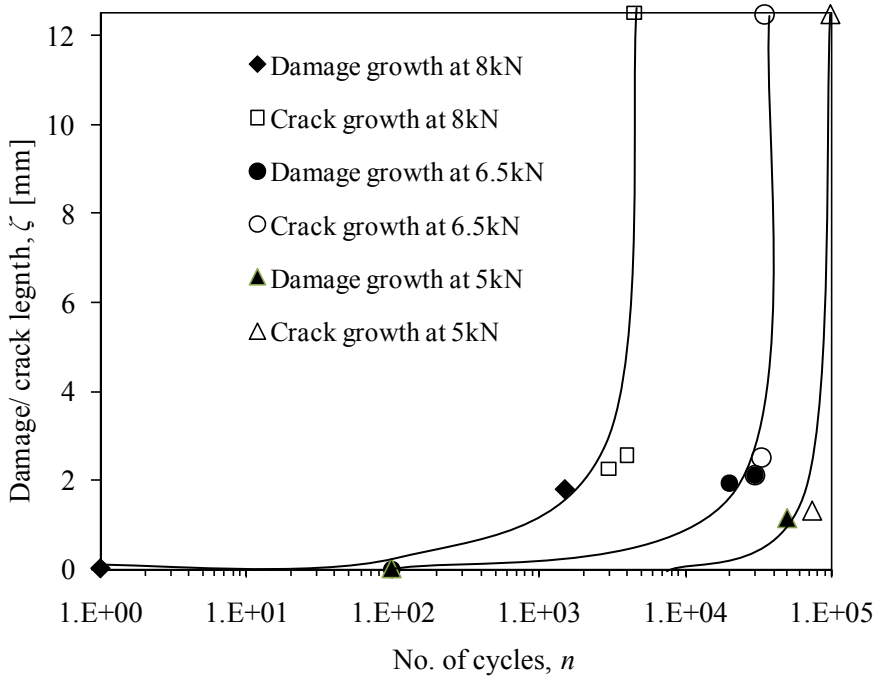

Fig. 5. Damage/ crack length as a function of number of cycles for different fatigue loads.

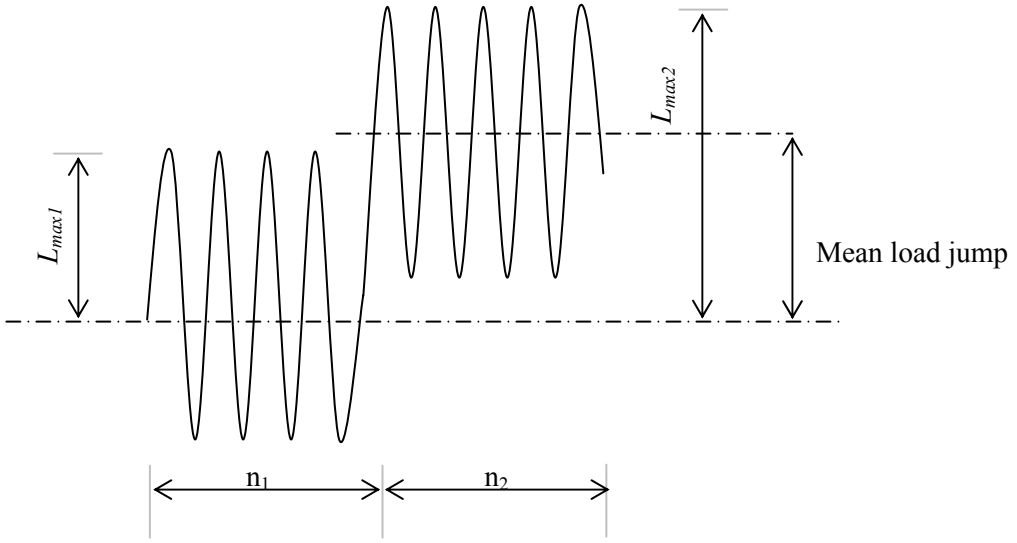

Type A spectra: $n_1/n_2 = 10/5$.

Type B spectra: $n_1/n_2 = 1000/5$.

Fig. 6. Two stages of block loading spectra used in the VAF experiments.

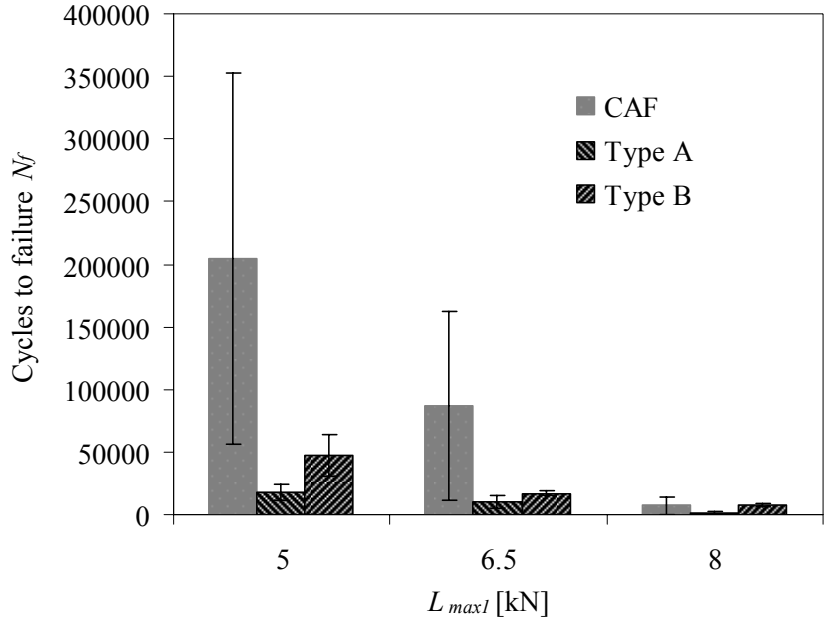

Fig. 7. Comparison of cycles to failure for CAF and VAF (Types A and B)

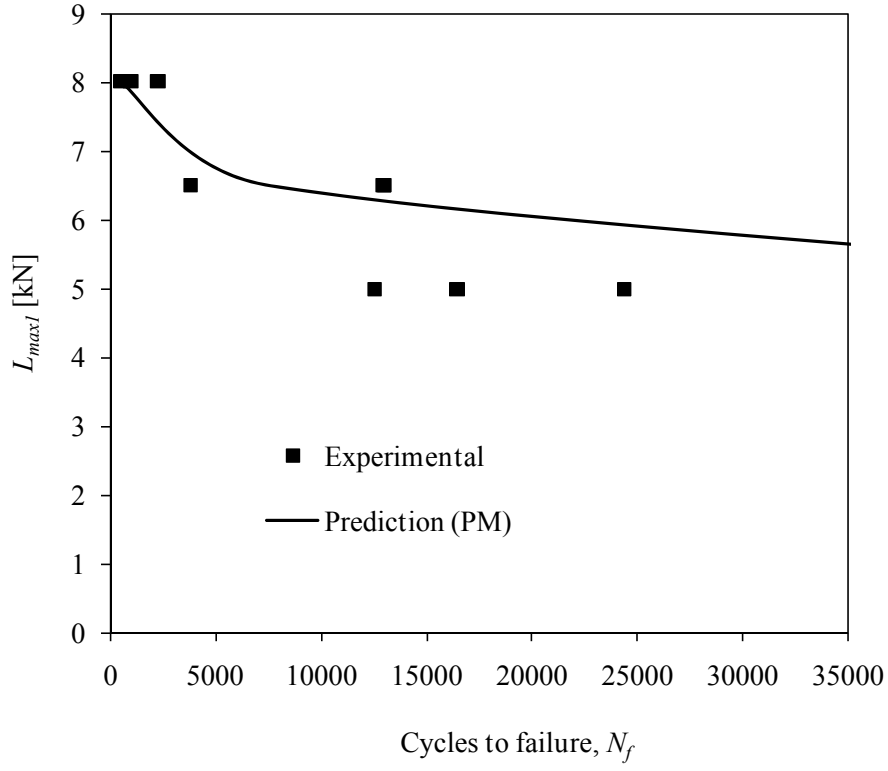

(a)

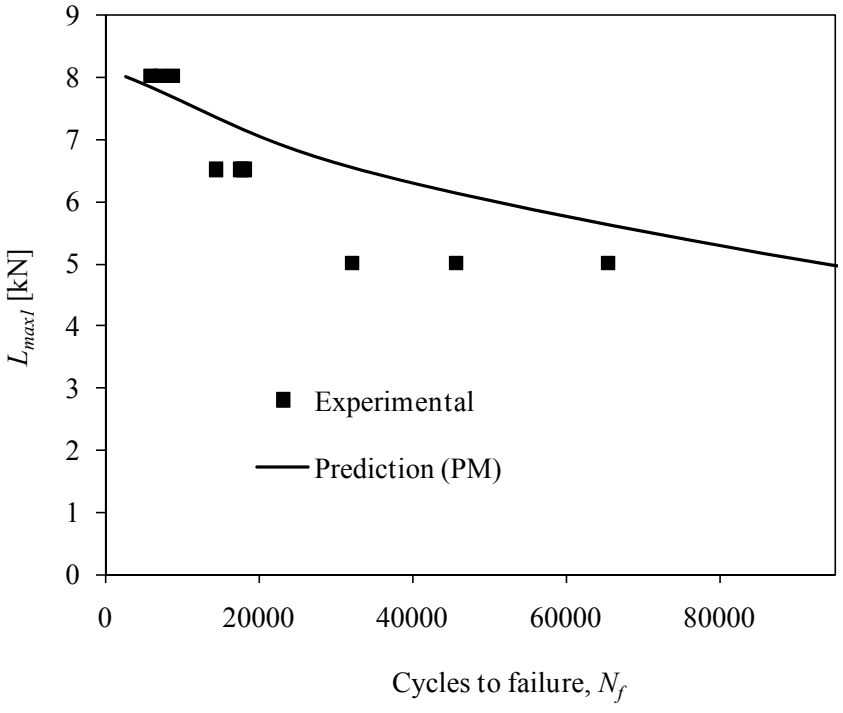

(b)

Fig. 8. Comparison between experimental and predicted L-N curves using the PM rule. (a) Type A spectra, (b) Type B spectra.

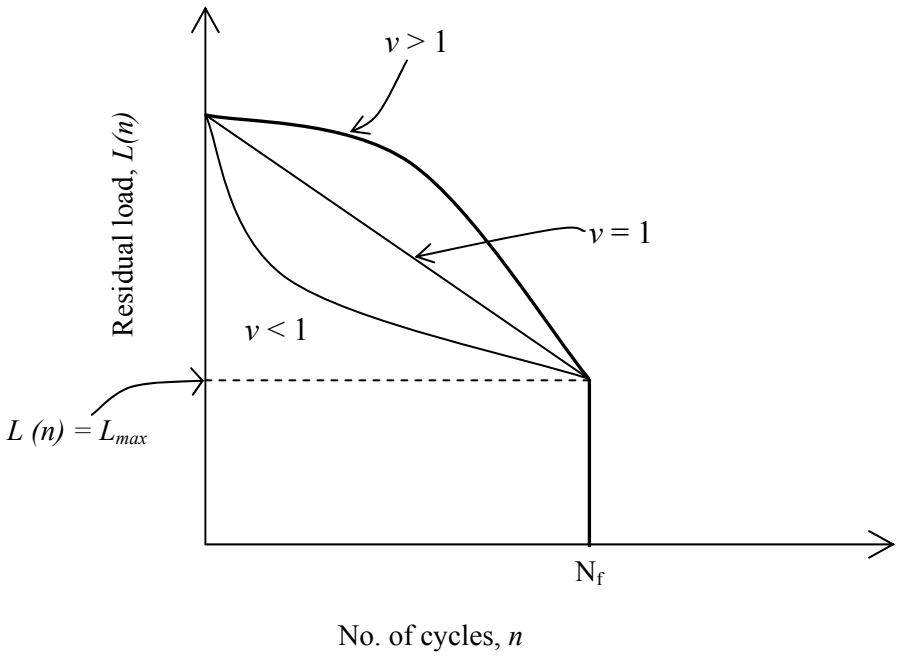

Fig. 9. Schematic representation of linear and non-linear strength wearout plots.

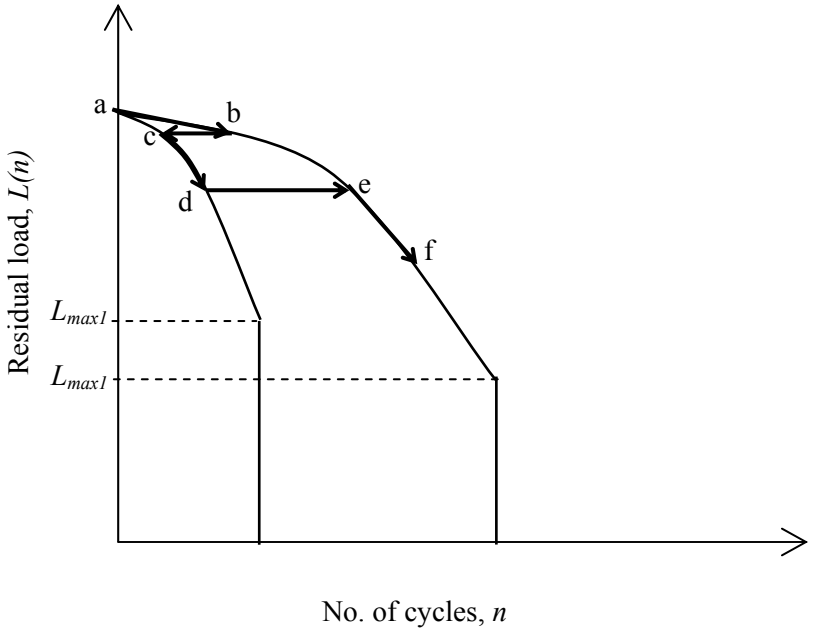

Fig. 10. VAF prediction using non-linear strength wearout curves with no interaction effects (NLSW method).

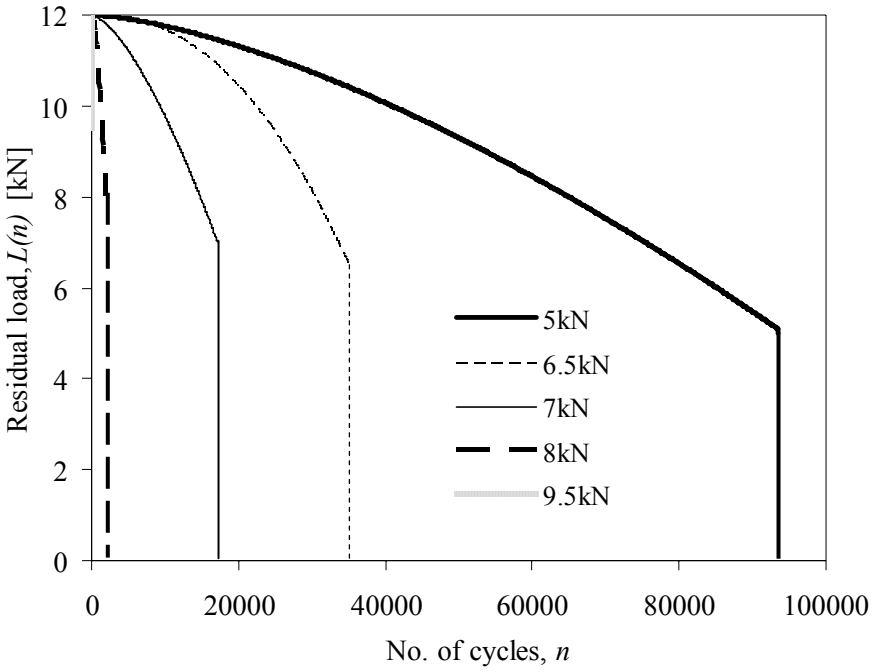

(a)

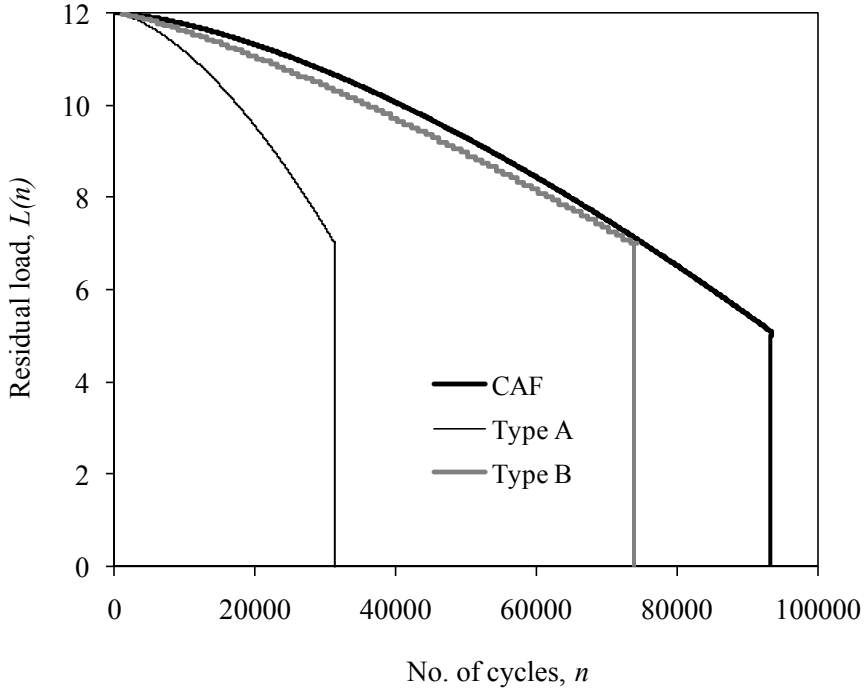

(b)

Fig. 11. (a) Strength wearout curves for CAF at various maximum fatigue loads, (b) comparison of strength wearout for CAF (max. fatigue load 5kN) and VAF using NLSW (both Types A and B, with L_{max1} = 5kN) .

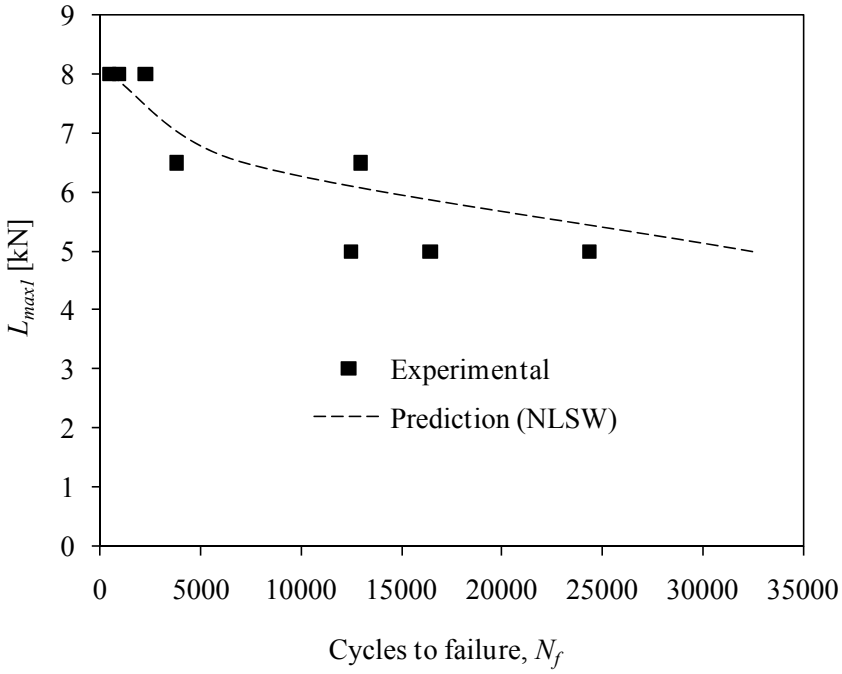

(a)

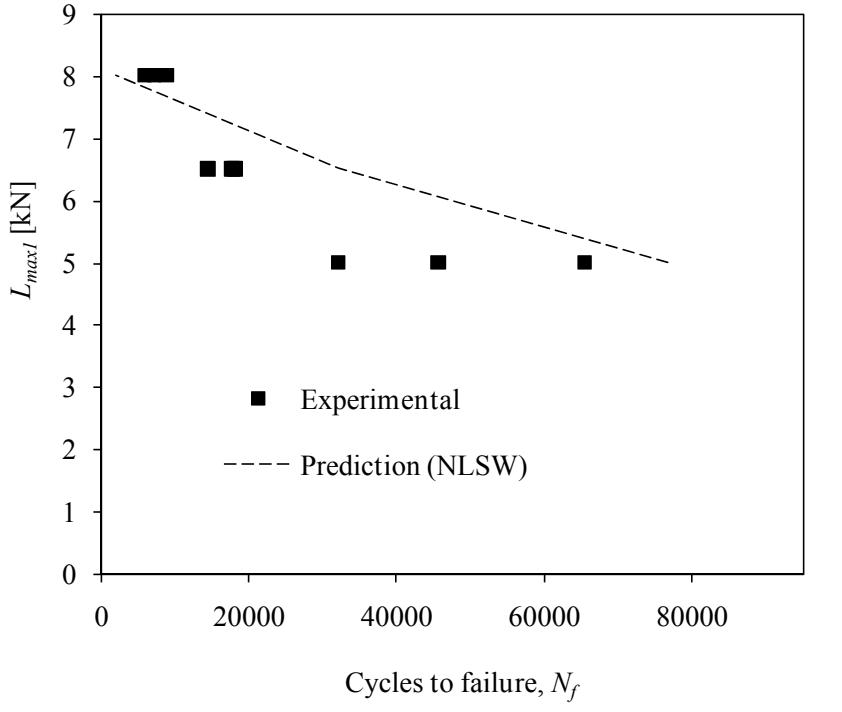

(b)

Fig. 12. Comparison between experimental and predicted L-N curves using the NLSW model. (a) Type A spectra, (b) Type B spectra.

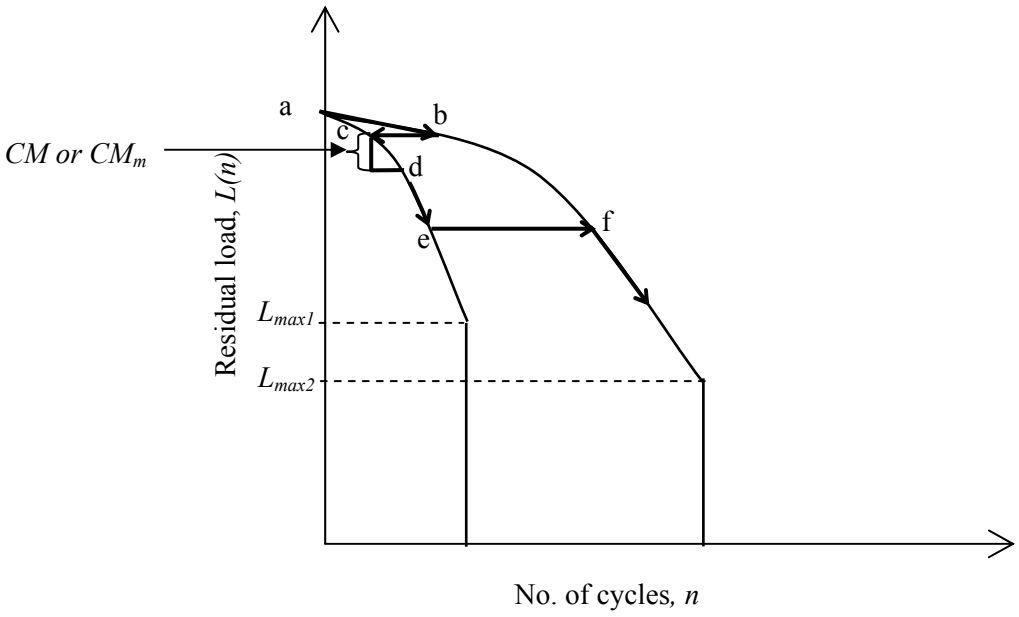

Fig. 13. Lifetime prediction model using strength wearout curves with cycle mix parameters to account for load interaction effects.

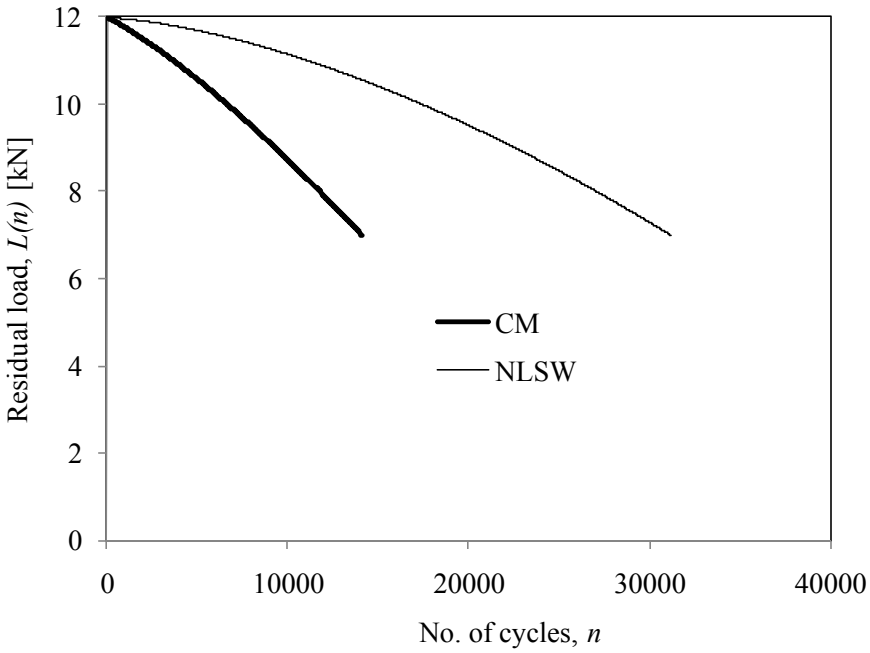

(a)

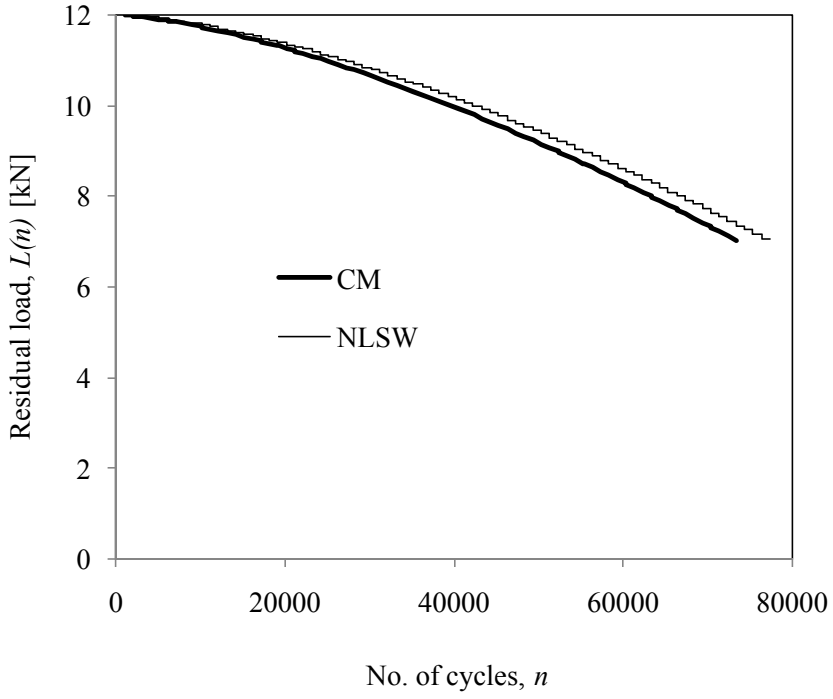

(a)

Fig. 14. Predicted strength wearout using CM and NLSW approaches (L_{max1} = 5kN) for (a) Type A spectrum and (b) Type B spectrum.

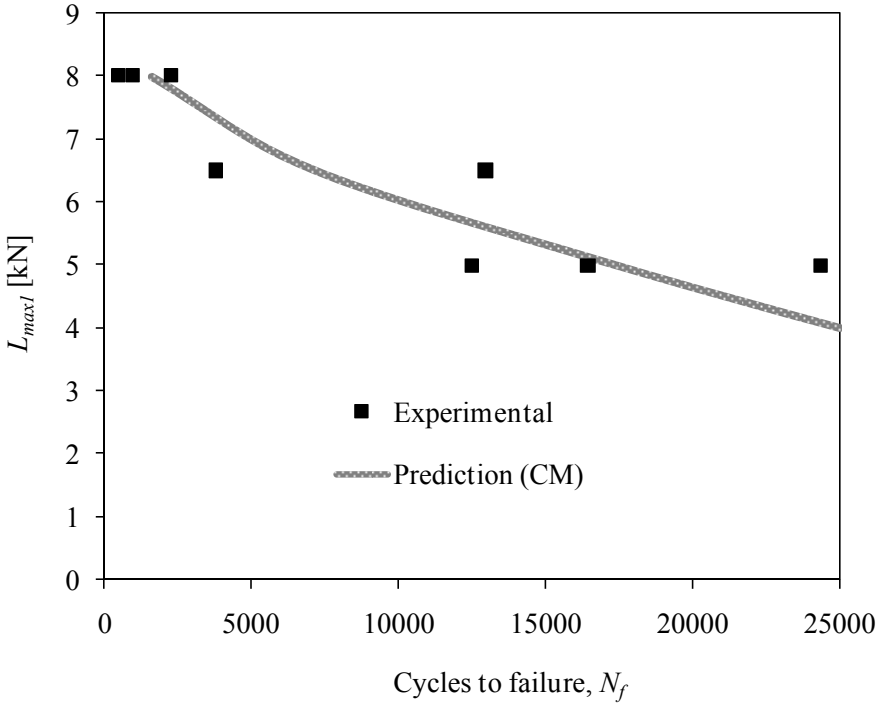

(a)

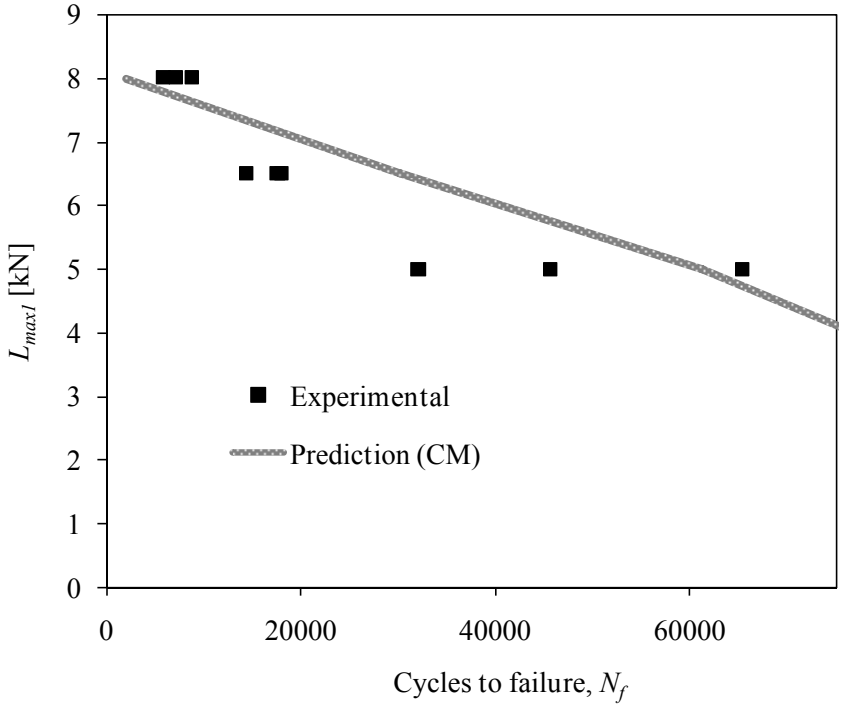

(b)

Fig. 15 Comparison between experimental and predicted L-N curves using the CM model. (a) Type A spectra, (b) Type B spectra.

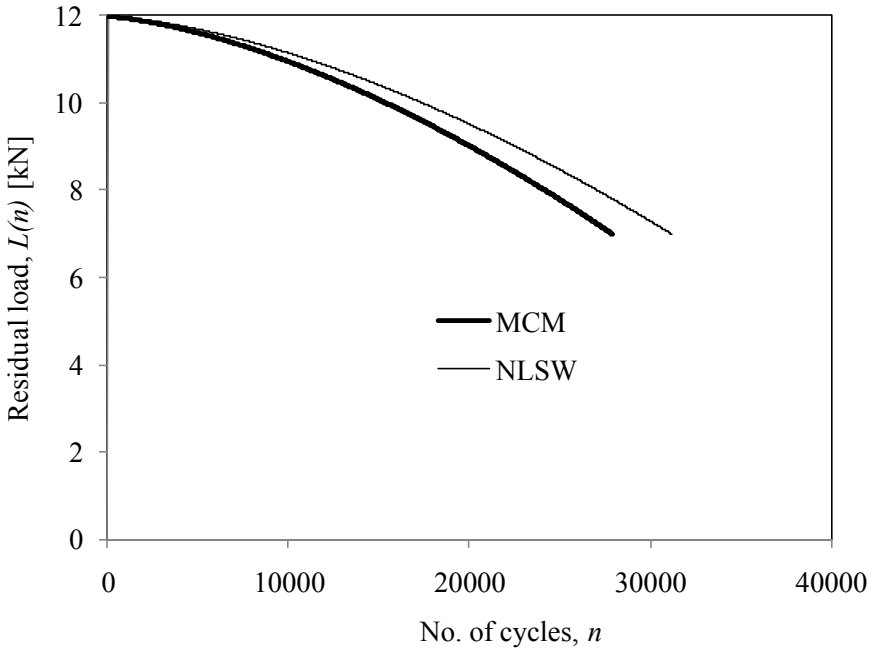

(a)

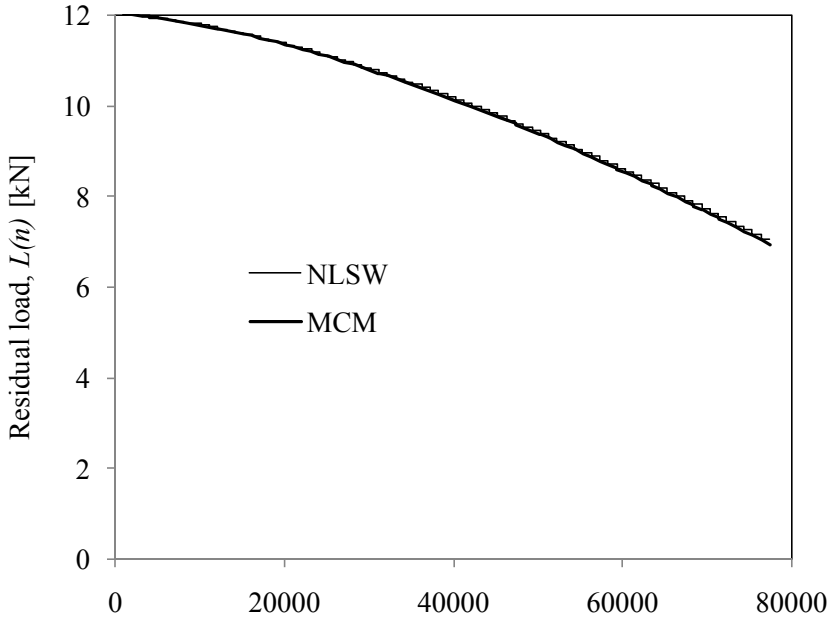

(b)

Fig. 16. Predicted strength wearout using MCM and NLSW approaches (L_{max1} = 5kN) for (a) Type A spectrum and (b) Type B spectrum.

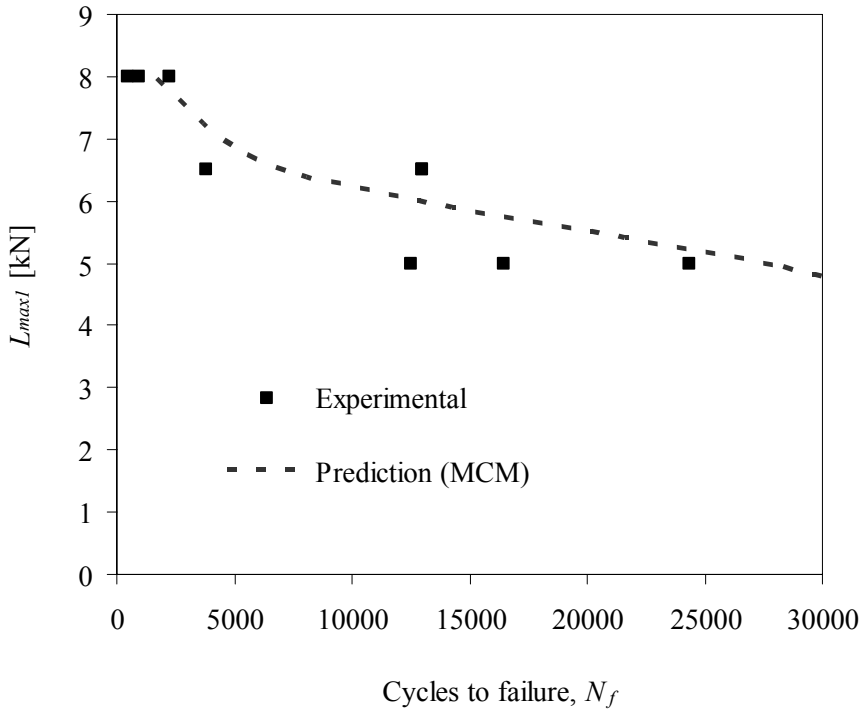

(a)

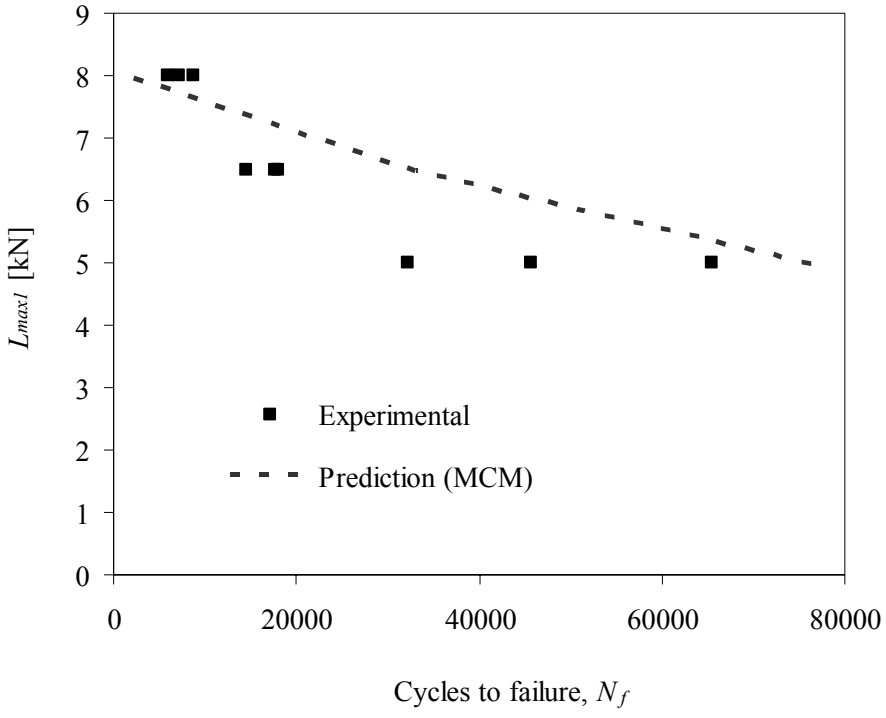

(b)

Fig. 17. Comparison between experimental and predicted L-N curves using the MCM model. (a) Type A spectra, (b) Type B spectra.

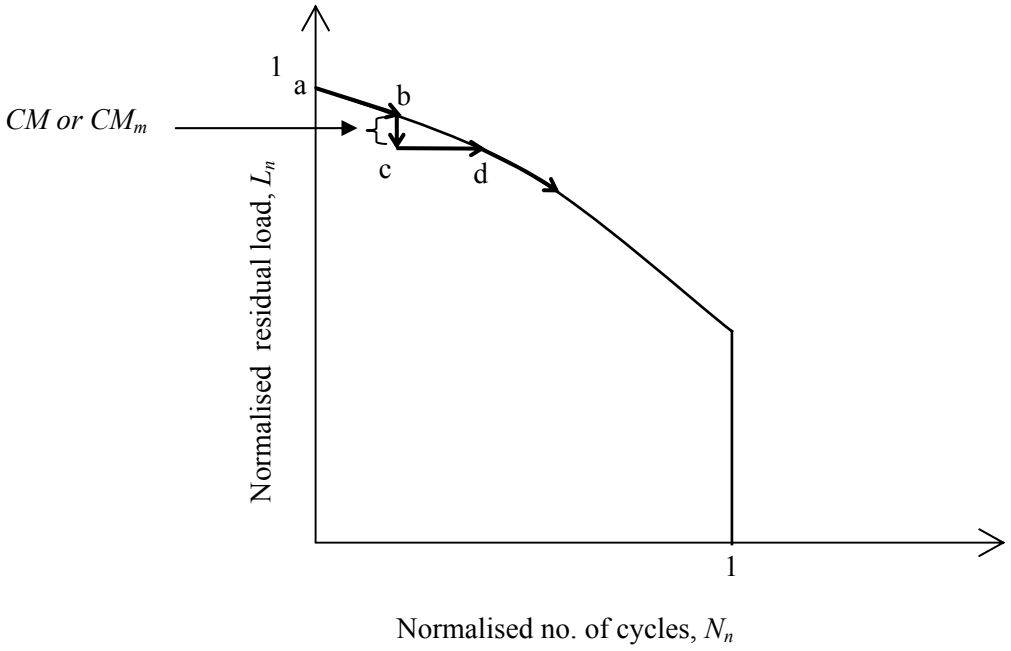

Fig. 18. Lifetime prediction model using normalised strength wearout curve with cycle mix parameters to account for load interaction effects.

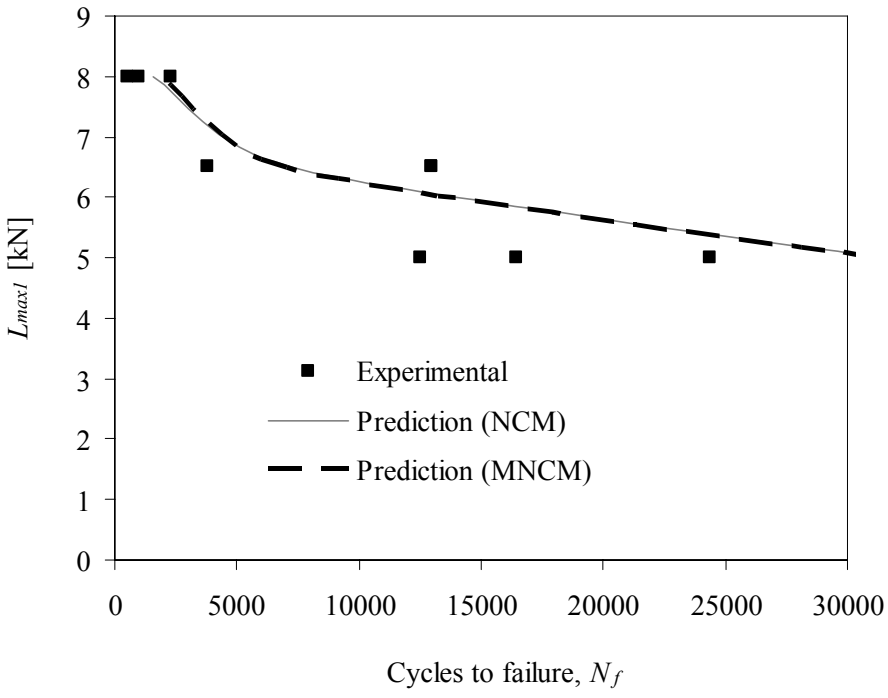

(a)

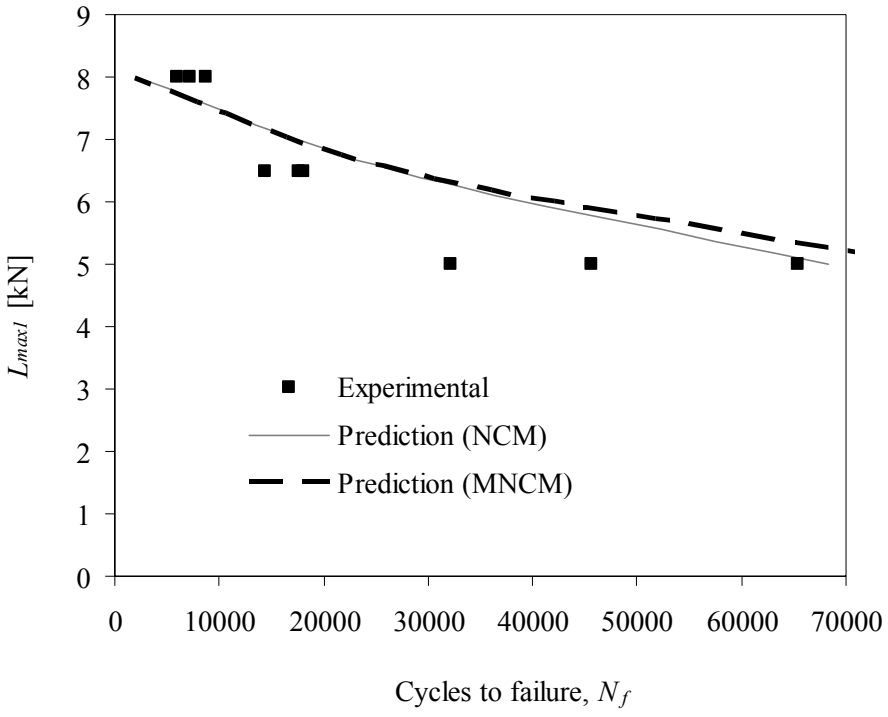

(b)

Fig. 19. Comparison between experimental and predicted L-N curves using the NCM and MNCM models. (a) Type A spectra, (b) Type B spectra.